The frequency-dependent conductivity of a saturated solution of $ZnBr_2$ in water: A molecular dynamics simulation

Gerald Löffler, Hellfried Schreiber, and Othmar Steinhauser[a)]
University of Vienna, Institute for Theoretical Chemistry, Molecular Dynamics Group, Währingerstaße 17/Parterre, A-1090 Wien, Austria

(Received 9 April 1996; accepted 9 May 1997)

The first part of this paper reviews the theory of the calculation of the frequency-dependent dielectric properties (i.e., conductivity and dielectric constant) of ionic solutions from computer simulations. Based on a 2.2-ns molecular dynamics simulation, the second part presents a detailed analysis of the various contributions to the frequency-dependent conductivity of a saturated solution of $ZnBr_2$ in water. We find evidence for two separate relaxation channels in the frequency-dependent conductivity, and a very low value for the static (i.e., zero frequency) conductivity, which is consistent with the high degree of ion association and the prevalence of electrically neutral ion clusters that we observe in this system. © *1997 American Institute of Physics.* [S0021-9606(97)50131-0]

I. INTRODUCTION

The dielectric properties of a piece of matter describe its reaction to an externally applied electric field. In the case of alternating fields, the dielectric properties depend on the frequency of the field. This paper deals with the calculation of the frequency-dependent dielectric properties of ionic solutions, which are the (frequency-dependent) *conductivity* and the (frequency-dependent) *dielectric constant* of the solution.

In an extensive series of papers, Caillol, Levesque, and Weis laid out the theory for the calculation of the dielectric properties of ionic solutions from molecular dynamics (MD) simulations.[1–6] Their theoretical results cover the most general case of polarizable ions in a polarizable solvent.[4] They performed several MD simulations of model systems, where ions were represented as charged Lennard-Jones particles and solvent molecules as Lennard-Jones particles with a dipole and a quadrupole moment, either being polar but nonpolarizable or being nonpolar but polarizable,[5] or being both polar and polarizable.[1] In general, their simulated solutions were of low to medium concentration. They stated the need for simulations of at least 10^6 time steps to be able to calculate the dielectric properties with sufficient accuracy.[5] They found the cross-correlation function $\langle \mathbf{M_W}(0)\mathbf{J_I}(t)\rangle$ between the total dipole moment of the water molecules and the total current of the ions—which is needed for the calculation of the dielectric properties of an ionic solution—to be essentially zero at all times.[1]

Later, Chandra, Wei, and Patey performed MD simulations of a wide range of model systems of aqueous ionic solutions and evaluated them according to the dielectric theory of Caillol *et al.*[7–10] Their systems consisted of ions modeled as charged Lennard-Jones particles and water molecules modeled as Lennard-Jones particles with a constant dipole moment (i.e., Stockmayer particles). They found characteristic variations of the dielectric properties with particle and charge density.[9,10] Again, the solutions were of low to medium concentration and the cross-correlation function $\langle \mathbf{M_W}(0)\mathbf{J_I}(t)\rangle$ was statistically zero in each case.[8]

Anderson *et al.*[11] performed MD simulations of the concentration dependence of the static dielectric constant. (i.e., at zero frequency) of aqueous NaCl solutions, using the simple point charge[12] (SPC) water model. They report good agreement of the expected decrease of the static dielectric constant with increasing ion concentration with experimental data.

In MD simulations of highly concentrated NaI solutions, where they modeled the water molecules as Stockmayer particles, Payne *et al.*[13] found that greater ion charges lead to the formation of ion clusters and to large deviations from the idealized Nernst–Einstein behavior. They neither calculated the conductivity nor the dielectric constant of the NaI solutions.

In an attempt to fill the apparent void of reasonably realistic simulations of highly concentrated aqueous ionic solutions, we performed a long (2.2-ns corresponding to 1.1×10^6 time steps) MD simulation of a saturated solution of $ZnBr_2$ in water (termed $ZnBr_2\cdot3H_2O$). In a recent paper, we evaluated the static and dynamic structure of this system and found good agreement with anomalous x-ray diffraction experiments.[14] Thus this simulation can be regarded as verified through comparison with experimental data. The high concentration of the solution enables us to have a closer look at the important cross-correlation function $\langle \mathbf{M_W}(0)\mathbf{J_I}(t)\rangle$.[8]

We will first review the computer-adapted dielectric theory of ionic solutions in a way that pronounces the influence of the actual treatment of the electrostatic interactions on the dielectric properties. This amendment extends the original derivation which was done by Caillol *et al.*[1,4] Then we will dissect the various contributions to the dielectric properties of $ZnBr_2\cdot3H_2O$ and ultimately present the frequency-dependent conductivity of this system. The calculation of the dielectric constant of the system is beyond what can be reaped from this 2.2-ns simulation.

a)Author to whom all correspondence should be addressed.

II. COMPUTER-ADAPTED DIELECTRIC THEORY

Computer-adapted dielectric theory makes dielectric properties consistently accessible from computer simulation. The three ingredients are linear response theory (Sec. II A), the phenomenological equations of matter (Sec. II B), and a unified approach to the electric field inside the simulation cell whatever treatment of the electrostatic interactions is employed in the simulation (Sec. II C).

The following recaps the derivation by Caillol *et al.*[1,4] and is similar in spirit to the work by Neumann and one of us (O.S.)[15–17] on the dielectric properties of pure liquids.

A. Linear response theory

If applied to the explanation of dielectric phenomena, linear response theory[18] deals with the response of a macroscopic system to an applied external electric field.

1. Macroscopic relations

On the macroscopic level, linear response theory assumes a linear relationship between the applied external field $\widetilde{\mathbf{E}_0}(\omega)$ and the ensemble average of an observable $\langle\widetilde{\mathbf{O}}(\omega)\rangle$:

$$\langle\widetilde{\mathbf{O}}(\omega)\rangle=\chi_{OP}(\omega)\widetilde{\mathbf{E}_0}(\omega). \tag{1}$$

Herein, $\chi_{OP}(\omega)$ is the (complex) *generalized susceptibility*, which describes the coupling of the observalbe $\mathbf{O}(t)$ to the *polarization* $\mathbf{P}(t)$ of the system.

2. Microscopic relations

According to linear response theory, the generalized susceptibility for an observable $\mathbf{O}(t)$ is defined as

$$\chi_{OP}(\omega)=\frac{1}{3kT}\left[\langle\mathbf{O}(0)\mathbf{M_W}(0)\rangle - i\omega\int_0^\infty\langle\mathbf{O}(0)\mathbf{M_W}(t)\rangle e^{-i\omega t}dt + \int_0^\infty\langle\mathbf{O}(0)\mathbf{J_I}(t)\rangle e^{-i\omega t}dt\right], \tag{2}$$

where $\mathbf{M_W}(t)$ is the *dipole moment of the water molecules*,

$$\mathbf{M_W}(t)=\sum_{i(\text{Waters})} q_i\mathbf{r_i}(t), \tag{3}$$

and $\mathbf{J_I}(t)$ is the *current of the ions*,

$$\mathbf{J_I}(t)\equiv\sum_{i(\text{Ions})} q_i\mathbf{v_i}(t)=\sum_{i(\text{Ions})} q_i\dot{\mathbf{r}}_\mathbf{i}(t)=\dot{\mathbf{M}}_\mathbf{I}(t). \tag{4}$$

Furthermore, $\langle A(0)B(t)\rangle$ denotes a time correlation function of the time-dependent quantities $A(t)$ and $B(t)$.

We used the fact that

$$\mathbf{P}(t)=\frac{1}{V}\sum_i q_i\mathbf{r_i}(t) \tag{5}$$

$$=\frac{1}{V}[\mathbf{M_W}(t)+\mathbf{M_I}(t)], \tag{6}$$

where the $\{q_i\}$ are the charges, which are located at the positions $\{\mathbf{r_i}\}$.

3. Special results

Equations (1) and (2), which are expressed in a general observable $\mathbf{O}(t)$, can be specialized for the *polarization of the water molecules* $\mathbf{P_W}(t)$

$$\mathbf{P_W}(t)=\frac{1}{V}\mathbf{M_W}(t) \tag{7}$$

and for the *current density of the ions* $\mathbf{i_I}(t)$

$$\mathbf{i_I}(t)=\frac{1}{V}\mathbf{J_I}(t), \tag{8}$$

giving

$$\langle\widetilde{\mathbf{P_W}}(\omega)\rangle=\chi_{P_WP}(\omega)\widetilde{\mathbf{E}_0}(\omega) \tag{9}$$

with

$$\chi_{P_WP}(\omega)=\frac{1}{3VkT}\left[\langle\mathbf{M_W}(0)\mathbf{M_W}(0)\rangle - i\omega\int_0^\infty\langle\mathbf{M_W}(0)\mathbf{M_W}(t)\rangle e^{-i\omega t}dt + \int_0^\infty\langle\mathbf{M_W}(0)\mathbf{J_I}(t)\rangle e^{-i\omega t}dt\right] \tag{10}$$

for the former, and

$$\langle\tilde{\mathbf{i}}_\mathbf{I}(\omega)\rangle=\chi_{i_IP}(\omega)\widetilde{\mathbf{E}_0}(\omega) \tag{11}$$

with

$$\chi_{i_IP}(\omega)=\frac{1}{3VkT}\left[-i\omega\int_0^\infty\langle\mathbf{M_W}(0)\mathbf{J_I}(t)\rangle e^{-i\omega t}dt + \int_0^\infty\langle\mathbf{J_I}(0)\mathbf{J_I}(t)\rangle e^{-i\omega t}dt\right] \tag{12}$$

for the latter.

In Eq. (12) we made use of the fact that $\langle\mathbf{M_W}(0)\mathbf{J_I}(0)\rangle=0$.

B. Phenomenological equations of matter

The phenomenological equations of matter are empirical relations—determined on macroscopic samples of matter—that can be regarded as the definition of the *frequency-dependent dielectric constant* $\epsilon(\omega)$

$$\widetilde{\mathbf{P_W}}(\omega)=\frac{\epsilon(\omega)-1}{4\pi}\widetilde{\mathbf{E}}(\omega) \tag{13}$$

and of the *frequency-dependent conductivity* $\sigma(\omega)$

$$\tilde{\mathbf{i}}_\mathbf{I}(\omega)=\sigma(\omega)\widetilde{\mathbf{E}}(\omega). \tag{14}$$

Both equations involve the frequency components of the so-called *Maxwell field* $\widetilde{\mathbf{E}}(\omega)$, which is the electric field acting inside the macroscopic piece of matter. The Maxwell field is, in general, different from the externally applied electric field

$\widetilde{\mathbf{E}_0}(\omega)$. Thus a comparison of Eqs. (13) and (9), as well as Eqs. (14) and (11), has to be postponed until the formalism relating $\widetilde{\mathbf{E}}(\omega)$ to $\widetilde{\mathbf{E}_0}(\omega)$ has been worked out in the next section.

C. Relating the Maxwell field $\tilde{\mathbf{E}}(\omega)$ to the external field $\widetilde{\mathbf{E}_0}(\omega)$

Quite intuitively, the field $\mathbf{E}(\mathbf{r},t)$ at some point $\mathbf{r}$ is the sum of the external field $\mathbf{E_0}(\mathbf{r},t)$ at that point, the field caused by all charges in the system (ions, in our case) at that point and the field caused by all dipoles in the system (water molecules, in our case) at that point:

$$\mathbf{E}(\mathbf{r},t)=\mathbf{E_0}(t)-\int_V \nabla_{\mathbf{r}}\Phi(\mathbf{r}-\mathbf{r}')\rho_I(\mathbf{r}',t)d\mathbf{r}' + \int_V \nabla_{\mathbf{r}}\nabla_{\mathbf{r}}\Phi(\mathbf{r}-\mathbf{r}')\mathbf{P_W}(\mathbf{r}',t)d\mathbf{r}'. \tag{15}$$

This formulation assumes that the external field is spatially homogeneous, hence $\mathbf{E_0}(\mathbf{r},t)=\mathbf{E_0}(t)$. The effective potential $\Phi(\mathbf{r})$ is the basis for the electrostatic interaction in the simulation, and can be any of the usually employed variants: potentials resulting from Coulomb interaction with or without cutoff, reaction field formulation, Ewald summation, other lattice summations, etc. $\rho_I(\mathbf{r},t)$ denotes the (continuous) charge density, and $\mathbf{P_W}(\mathbf{r},t)$ the (continuous) dipole density. Due to their zero net charge, the water molecules enter into this formula only through the dipolar contribution. Similarly, ions are treated as point charges and enter into this formula only through the charge distribution.

The double gradient of the electrostatic potential, which is a 3×3 matrix by nature, is called the *T tensor*:

$$\overleftrightarrow{T}(\mathbf{r})\equiv\nabla_{\mathbf{r}}\nabla_{\mathbf{r}}\Phi(\mathbf{r}). \tag{16}$$

To get an expression for the Maxwell field, we identify the whole simulation system with the macroscopic piece of matter for which to calculate the Maxwell field, and consequently average the spatially resolved field $\mathbf{E}(\mathbf{r},t)$ over the simulation system:

$$\mathbf{E}(t)=\frac{1}{V}\int_V \mathbf{E}(\mathbf{r},t)\mathbf{dr} \tag{17}$$

$$=\mathbf{E_0}(t)-\frac{1}{V}\int_V\int_V \nabla_{\mathbf{r}}\Phi(\mathbf{r}-\mathbf{r}')\rho_I(\mathbf{r}',t)d\mathbf{r}'d\mathbf{r} + \frac{1}{V}\int_V\int_V \overleftrightarrow{T}(\mathbf{r}-\mathbf{r}')\mathbf{P_W}(\mathbf{r}',t)d\mathbf{r}'d\mathbf{r}. \tag{18}$$

When we now switch from the variable $\mathbf{r}$ to $\mathbf{r}''=\mathbf{r}-\mathbf{r}'$ it is essential to realize that due to the *periodic boundary conditions* that are used routinely in simulations of this kind, $\mathbf{r}''\in V$. Conversely, a simulation that is performed without periodic boundary conditions cannot be evaluated with the computer-adapted dielectric theory as described here

$$\mathbf{E}(t)=\mathbf{E_0}(t)-\frac{1}{V}\int_V \nabla_{\mathbf{r}''}\Phi(\mathbf{r}'')d\mathbf{r}''\int_V \rho_I(\mathbf{r}',t)d\mathbf{r}' + \frac{1}{V}\int_V \overleftrightarrow{T}(\mathbf{r}'')d\mathbf{r}''\int_V \mathbf{P_W}(\mathbf{r}',t)d\mathbf{r}'. \tag{19}$$

Now, since the simulated system has to be neutral (a requirement dictated by common sense and the laws of electrostatics),

$$\int_V \rho_I(\mathbf{r},t)d\mathbf{r}=0. \tag{20}$$

Furthermore, the integral of the T tensor over the simulation system is for *isotropic systems*, a multiple of the unit-tensor $\overleftrightarrow{I}$, and can therefore be characterised by a scalar ϵ_{RF}, such that[15]

$$\int_V \overleftrightarrow{T}(\mathbf{r})d\mathbf{r}\equiv\left[\frac{4\pi}{3}\frac{2(\epsilon_{\mathrm{RF}}-1)}{2\epsilon_{\mathrm{RF}}+1}-\frac{4\pi}{3}\right]\overleftrightarrow{I}. \tag{21}$$

The name ϵ_{RF} stems from the fact that, if the reaction field formalism is taken as the basis for electrostatic interactions, the integral of the T tensor has exactly the above appearance, with ϵ_{RF} being the dielectric constant of the dielectric continuum which causes the reaction field. However, for the other possible electrostatic potentials, ϵ_{RF} should merely be regarded as a parameter that can be used to characterize the integral of the T tensor.

Additionally, the spatial average of the dipole density in Eq. (19) can be expressed in terms of the polarization of the water molecules:

$$\frac{1}{V}\int_V \mathbf{P_W}(\mathbf{r},t)d\mathbf{r}=\mathbf{P_W}(t). \tag{22}$$

This leads to an expression for the (time-dependent) Maxwell field $\mathbf{E}(t)$ in the simulation system:

$$\mathbf{E}(t)=\mathbf{E_0}(t)+\frac{4\pi}{3}\left[\frac{2(\epsilon_{\mathrm{RF}}-1)}{2\epsilon_{\mathrm{RF}}+1}-1\right]\mathbf{P_W}(t). \tag{23}$$

Taking frequency components and using Eq. (13), we find

$$\widetilde{\mathbf{E}}(\omega)=\widetilde{\mathbf{E}_0}(\omega)+\frac{4\pi}{3}\left[\frac{2(\epsilon_{\mathrm{RF}}-1)}{2\epsilon_{\mathrm{RF}}+1}-1\right]\frac{\epsilon(\omega)-1}{4\pi}\widetilde{\mathbf{E}}(\omega), \tag{24}$$

which can be rearranged to give the desired relation between the external field $\widetilde{\mathbf{E}_0}(\omega)$ and the Maxwell field $\widetilde{\mathbf{E}}(\omega)$:

$$\frac{\widetilde{\mathbf{E}}(\omega)}{\widetilde{\mathbf{E}_0}(\omega)}=\frac{2\epsilon_{\mathrm{RF}}+1}{2\epsilon_{\mathrm{RF}}+\epsilon(\omega)}. \tag{25}$$

Please note that the precise electrostatic interaction we use for the simulation of the system enters into this equation only through the constant ϵ_{RF}, which can be calculated from Eq. (21). On the other hand, $\epsilon(\omega)$ is the frequency-dependent dielectric constant of the system, which is one of the desired end results of this theory.

D. Putting it all together

Finally, we are in a position to give explicit expressions for the dielectric properties of interest.

1. The frequency-dependent dielectric constant $\epsilon(\omega)$

Using Eqs. (9), (13), and (25):

$$\frac{\epsilon(\omega)-1}{4\pi}=\left[1-\frac{4\pi\chi_{P_{W^P}}(\omega)}{2\epsilon_{\mathrm{RF}}+1}\right]^{-1}\chi_{P_{W^P}}(\omega), \tag{26}$$

where $\chi_{P_{W^P}}$ is given by Eq. (10) and ϵ_{RF} by Eq. (21).

2. The frequency-dependent conductivity $\sigma(\omega)$

Using Eqs. (11), (14), (25), and (26):

$$\sigma(\omega)=\left[1-\frac{4\pi\chi_{P_{W^P}}(\omega)}{2\epsilon_{\mathrm{RF}}+1}\right]^{-1}\chi_{i_{I^P}}(\omega), \tag{27}$$

where $\chi_{P_{W^P}}$ given by Eq. (10), $\chi_{i_{I^P}}$ by Eq. (12), and ϵ_{RF} by Eq. (21).

E. The role of ϵ_{RF}

The parameter ϵ_{RF} can be calculated for every possible effective electrostatic potential used in MD simulations.[15] Since the simulation presented in this work was done with the Ewald potential, we will concentrate on this potential here. It was found[15] that for the Ewald summation,

$$\epsilon_{\mathrm{RF}}=\frac{2+Q}{2(1-Q)}, \tag{28}$$

where the constant Q is determined by the parameters r_C (the cutoff radius for the real part of the Ewald potential) and η (the so-called decay parameter of the Ewald summation that determines the relative contributions of real part and Fourier space part) of the actual implementation of the Ewald summation:

$$Q=\int_0^{r_C}\left(\frac{\eta}{\sqrt{\pi}}\right)^3 e^{-\eta^2 r^2}4\pi r^2 dr. \tag{29}$$

Since the integrand in this expression is just a normalized Gaussian,

$$\lim_{r_C\to\infty} Q=\lim_{\eta\to\infty} Q=1, \tag{30}$$

and consequently

$$\lim_{r_C\to\infty} \epsilon_{\mathrm{RF}}=\lim_{\eta\to\infty} \epsilon_{\mathrm{RF}}\to\infty. \tag{31}$$

Because a real implementation of the Ewald summation will never truly achieve this limit of $\epsilon_{\mathrm{RF}}=\infty$, it is representative for the *ideal Ewald summation*. However, an infinite value of ϵ_{RF} has important implications for the calculation of the dielectric constant and the conductivity according to Eqs. (26) and (27):

$$\frac{\epsilon(\omega)-1}{4\pi}=\chi_{P_{W^P}}(\omega), \tag{32}$$

$$\sigma(\omega)=\chi_{i_{I^P}}(\omega). \tag{33}$$

This can also be understood by inserting an infinite ϵ_{RF} into Eq. (25), which shows that the externally applied electric field is in this case identical to the Maxwell field, from which follows, that Eqs. (13) and (9), as well as Eqs. (14) and (11), can now be compared directly.

A comparison of Eqs. (32) and (26) and (33) and (27), respectively, shows that the susceptibilities $\chi_{P_{W^P}}(\omega)$ and $\chi_{i_{I^P}}(\omega)$ reach their maximum value if $\epsilon_{\mathrm{RF}}=\infty$. For all other values $\epsilon_{\mathrm{RF}}<\infty$, the factor $[1-4\pi\chi_{P_{W^P}}(\omega)/2\epsilon_{\mathrm{RF}}+1]^{-1}$ becomes greater than one, and thus if the dielectric constant and conductivity are to remain the same—because they are universal intrinsic properties of matter—the susceptibilities have to become smaller.

Only in the case of the ideal Ewald potential is the conductivity $\sigma(\omega)$ independent of the dielectric constant as represented by the susceptibility $\chi_{P_{W^P}}(\omega)$ [cf. Eqs. (33) and (27)].

In this work we tried to realize an ideal implementation of the Ewald summation as well as possible, with the consequence, that we do not have to determine the susceptibility $\chi_{P_{W^P}}(\omega)$ in order to calculate the conductivity $\sigma(\omega)$.

III. MOLECULAR DYNAMICS SIMULATION

The following results are based on a 2.2-ns MD simulation of $ZnBr_2\cdot 3H_2O$ using Lennard-Jones interaction and Ewald summation. The details of the simulation are as follows:

- System size: $(3.461\ \mathrm{nm})^3$.
- The system contained 233 units $ZnBr_2$ and 663 SPC (simple point charge) water molecules,[12] all together 2688 atoms.
- Temperature: 300 K, held constant with coupling to an external heat bath.[19]
- Time step for the integration of the Newtonian equations of motion: 2 fs.
- Usage of a constraint algorithm for the maintenance of the geometry of water molecules.[20] Thus the dipole moment of each water molecule is constant, but water molecules do not act as point dipoles (as in the case of a Stockmayer system) but as collections of point charges.
- Cutoff for Lennard-Jones interaction: 1.0 nm.
- Ewald summation[21–23] for the electrostatic interactions using a decay parameter $\eta=2.179\,82\ \mathrm{nm}^{-1}$, 230 k-vectors, and a cutoff for the real part of the Ewald interaction of 1.2 nm.
- The spatial extension of atoms was described by the Lennard-Jones potential $U_{LJ}=A_{ij}/r^{12}-B_{ij}/r^6$, where the pair-specific parameters A_{ij} and B_{ij} were calculated from atom-specific parameters: $A_{ij}=A_i' A_j'$ and $B_{ij}=B_i' B_j'$. These atom-specific parameters were—with the exception of the Br− parameters—taken from the general purpose force field of the GROMOS package[24] and are summarized in Table I.

TABLE I. The atom-specific parameters for the Lennard-Jones interaction. See text for details.

Atom type	Partner	A'/kJ$^{1/2}$ mol$^{-1/2}$ nm^6	B'/kJ$^{1/2}$ mol$^{-1/2}$ nm^3
Zn^{2+}	Zn^{2+}, Br^-, O, H	0.9716×10^{-4}	0
Br^-	Zn^{2+}, Br^-, O, H	0.1544×10^{-1}	0.132 96
O	Zn^{2+}, O, H	0.1623×10^{-2}	0.051 16
O	Br^-	0.8615×10^{-3}	0.047 56
H	Zn^{2+}, Br^-, O, H	0	0

GROMOS does not give parameters for Br^-, so we derived the Br^- parameters from the known Cl^- parameters.

• The partial charges on the atoms of water were according to the SPC model[12] -0.82 acu on O and $+0.41$ acu on each H (acu means atomic charge units). The charges of Zn^{2+} and Br^- were, of course, $+2$ acu and -1 acu, respectively.

Recently,[14] we compared the static structure of $ZnBr_2\cdot3H_2O$ as this simulation suggests it to the results of anomalous x-ray diffraction experiments of $ZnBr_2\cdot3H_2O$ and found good agreement within the experimental uncertainties. Judged by Eqs. (28) and (29), the implementation we used for the Ewald summation comes close to the ideal of $\epsilon_{RF}=\infty$. For that case Eq. (33) states that the frequency-dependent conductivity $\sigma(\omega)$ is equal to the susceptibility $\chi_{i_I P}(\omega)$ given by Eq. (12). Following the latter, we will first analyze the two correlation functions $\langle \mathbf{M_W}(0)\mathbf{J_I}(t)\rangle$ and $\langle \mathbf{J_I}(0)\mathbf{J_I}(t)\rangle$ before combining them to $\sigma(\omega)$ itself.

A. The cross-correlation function $\langle \mathbf{M_W}(0)\mathbf{J_I}(t)\rangle$

The cross-correlation function $\langle \mathbf{M_W}(0)\mathbf{J_I}(t)\rangle$ appears in the expressions for both susceptibilities, $\chi_{P_W P}(\omega)$ [Eq. (10)] and $\chi_{i_I P}(\omega)$ [Eq. (12)], because it describes the coupling of the dipole moment $\mathbf{M_W}$ to the current $\mathbf{J_I}$. Since the current can be separated into the current $\mathbf{J}_{Zn}(t)$ of the Zn^{2+} ions and the current $\mathbf{J}_{Br}(t)$ of the Br^- ions

$$\mathbf{J_I}(t)=\sum_{i(\text{Ions})} q_i\mathbf{v_i}(t)$$

$$=q_{Zn}\sum_{i(Zn)}\mathbf{v_i}(t)+q_{Br}\sum_{j(Br)}\mathbf{v_j}(t) \tag{34}$$

$$=\mathbf{J}_{Zn}(t)+\mathbf{J}_{Br}(t); \tag{35}$$

the same can be done for the cross-correlation function:

$$\langle \mathbf{M_W}(0)\mathbf{J_I}(t)\rangle=\langle \mathbf{M_W}(0)\mathbf{J}_{Zn}(t)\rangle+\langle \mathbf{M_W}(0)\mathbf{J}_{Br}(t)\rangle. \tag{36}$$

The cross-correlation function and its two contributions are shown in Fig. 1. $\langle \mathbf{M_W}(0)\mathbf{J}_{Zn}(t)\rangle$ and $\langle \mathbf{M_W}(0)\mathbf{J}_{Br}(t)\rangle$ decay slowly toward zero within the accessible time window of this simulation. The different signs of these two functions is due to the different sign of the charges of Zn^{2+} and Br^{-1}. Taking this into account, we see that the sum of the velocities of the Zn^{2+} ions and the sum of the velocities of the Br^- ions are parallel to each other and antiparallel to the dipole moment of the water molecules. $\langle \mathbf{M_W}(0)\mathbf{J_I}(t)\rangle$, as the sum of these two functions, stays almost constant throughout the period of

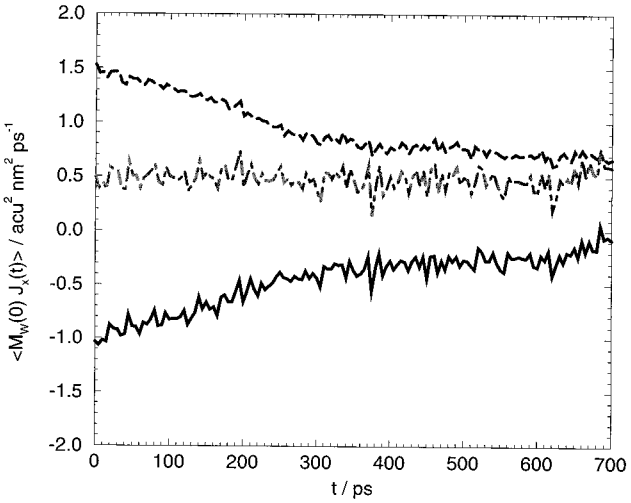

FIG. 1. The cross-correlation function $\langle \mathbf{M_W}(0)\mathbf{J_I}(t)\rangle$ (dot-dashed, middle line) and its two contributions $\langle \mathbf{M_W}(0)\mathbf{J}_{Zn}(t)\rangle$ (solid, bottom line) and $\langle \mathbf{M_W}(0)\mathbf{J}_{Br}(t)\rangle$ (dashed, top line).

700 ps. In a perfect simulation, the static value $\langle \mathbf{M_W}(0)\mathbf{J_I}(0)\rangle$ should be zero. This is not the case in this simulation, because $\mathbf{M_W}(t)$ varies very slowly and is not sufficiently sampled by a 2.2-ns simulation. Consequently, $\langle \mathbf{M_W}(0)\mathbf{J_I}(t)\rangle$—as the only correlation function in this work that involves $\mathbf{M_W}(t)$—can only be taken semiquantitatively. Under these circumstances, $\langle \mathbf{M_W}(0)\mathbf{J_I}(t)\rangle$ can be regarded to be essentially zero for all values of t, which is consistent with results by Chandra, Wei, and Patey.[8] We would like to stress that $\langle \mathbf{M_W}(0)\mathbf{J_I}(t)\rangle$ is the only correlation function presented in this paper that would benefit appreciably from better sampling.

The correlation functions shown in Fig. 1 give an impression of the correlation of the bulk properties $\mathbf{M_W}$ and $\mathbf{J}_{Zn}$ or $\mathbf{J}_{Br}$, respectively. The other extreme in the coupling of a dipole moment to a current, which can help in understanding the correlation of the motion of water molecules and ions, is the correlation between the property of a single particle and the property of the first coordination shell around this particle. In particular, we calculated the correlation function $\langle q_{Zn}\mathbf{v}_{Zn}(0)\mathbf{M}_{\mathbf{W}_{shell}}(t)\rangle$ between the current of a Zn^{2+} ion and the dipole moment of the water molecules in the first coordination shell around this Zn^{2+} ion. Analogously, we calculated the correlation function $\langle q_{Br}\mathbf{v}_{Br}(0)\mathbf{M}_{\mathbf{W}_{shell}}(t)\rangle$ between the current of a Br^- ion and the dipole moment of the water molecules in the first coordination shell around this Br^- ion.

These correlation functions are shown in Fig. 2. The first coordination shell around a particle was calculated with the Voronoi algorithm,[25–27] as extensively described in Ref. 14. $\langle q_{Zn}\mathbf{v}_{Zn}(0)\mathbf{M}_{\mathbf{W}_{shell}}(t)\rangle$ is positive, meaning that the dipole moment of the water molecules around a Zn^{2+} ion is parallel to the current (or velocity) of this Zn^{2+} ion. This is in contrast to the corresponding bulk properties, where $\mathbf{M_W}$ is antiparallel to $\mathbf{J}_{Zn}$. Similarly, $\langle q_{Br}\mathbf{v}_{Br}(0)\mathbf{M}_{\mathbf{W}_{shell}}(t)\rangle$ is negative, so that the dipole moment of the water molecules around a Br^- ion is parallel to the velocity of this Br^- ion. In short,

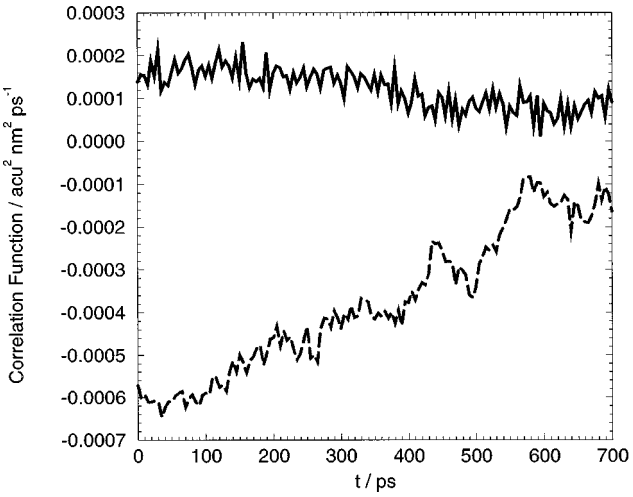

FIG. 2. Two correlation functions describing the correlation between the current of a particle and the dipole monent of the first coordination shell around this particle:$\langle q_{\mathrm{Zn}}\mathbf{v}_{\mathrm{Zn}}(0)\mathbf{M}_{\mathbf{W}_{\mathrm{shell}}}(t)\rangle$ (solid, top line) and $\langle q_{\mathrm{Br}}\mathbf{v}_{\mathrm{Br}}(0)\mathbf{M}_{\mathbf{W}_{\mathrm{shell}}}(t)\rangle$ (dashed, bottom line).

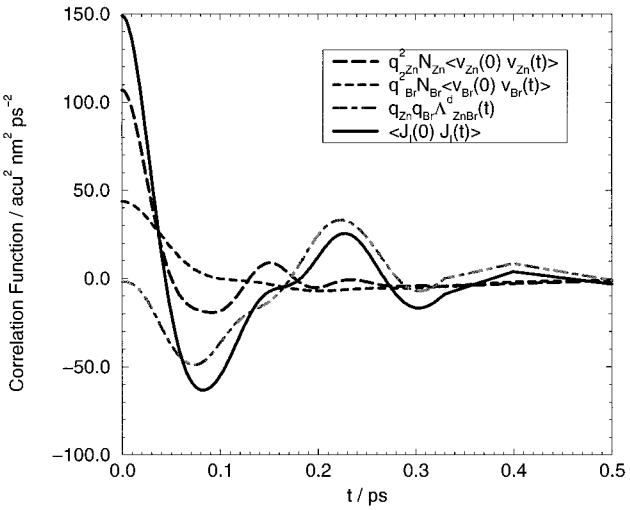

FIG. 3. The current autocorrelation function $\langle \mathbf{J_I}(0)\mathbf{J_I}(t)\rangle$ and its subdivision into the reference frame independent correlation functions $q^2_{\mathrm{Zn}}N_{\mathrm{Zn}}\langle \mathbf{v}_{\mathrm{Zn}}(0)\mathbf{v}_{\mathrm{Zn}}(t)\rangle$, $q^2_{\mathrm{Br}}N_{\mathrm{Br}}\langle \mathbf{v}_{\mathrm{Br}}(0)\mathbf{v}_{\mathrm{Br}}(t)\rangle$, and $q_{\mathrm{Zn}}q_{\mathrm{Br}}\Lambda^d_{\mathrm{ZnBr}}(t)$.

we observe an antiparallel orientation of the sum of all water dipole moments to the sum of all ion velocities (the macroscopic situation), but a parallel orientation of the sum of the water dipole moments in the first coordination shell around an ion to the velocity of this ion (the microscopic situation). In both cases—the collective and the atomistic—the long relaxation times of the cross-correlation functions prove a strong coupling of the translational motion of the ions to the rotational motion of the water molecules.

B. The autocorrelation function $\langle \mathbf{J_I}(0)\mathbf{J_I}(t)\rangle$

As $\langle \mathbf{M_W}(0)\mathbf{J}_{\mathrm{Zn}}(t)\rangle$ was found to be negligible, the autocorrelation function of the current of the ions $\langle \mathbf{J_I}(0)\mathbf{J_I}(t)\rangle$ determines the frequency-dependent conductivity according to Eqs. (33) and (12). We will analyze the contributions to $\langle \mathbf{J_I}(0)\mathbf{J_I}(t)\rangle$ in the following:

Substituting Eq. (34) into $\langle \mathbf{J_I}(0)\mathbf{J_I}(t)\rangle$ using the number of Zn^{2+} ions ($N_{\mathrm{Zn}}=233$), the number of Br^- ions ($N_{\mathrm{Br}}=466$), and the charge of the ions ($q_{\mathrm{Zn}}=2$ and $q_{\mathrm{Br}}=-1$, respectively) gives

$$\langle \mathbf{J_I}(0)\mathbf{J_I}(t)\rangle = q^2_{\mathrm{Zn}}N_{\mathrm{Zn}}\langle \mathbf{v}_{\mathrm{Zn}}(0)\mathbf{v}_{\mathrm{Zn}}(t)\rangle + q^2_{\mathrm{Br}}N_{\mathrm{Br}}\langle \mathbf{v}_{\mathrm{Br}}(0)\mathbf{v}_{\mathrm{Br}}(t)\rangle + q_{\mathrm{Zn}}q_{\mathrm{Br}}\Lambda^d_{\mathrm{ZnBr}}(t). \tag{37}$$

The first term on the right-hand side involves the velocity autocorrelation function$\langle \mathbf{v}_{\mathrm{Zn}}(0)\mathbf{v}_{\mathrm{Zn}}(t)\rangle$ of the Zn^{2+} ions; the second term involves the velocity autocorrelation function $\langle \mathbf{v}_{\mathrm{Br}}(0)\mathbf{v}_{\mathrm{Br}}(t)\rangle$ of the Br^- ions, and the third term contains the correlation function $\Lambda^d_{\mathrm{ZnBr}}(t)$ that measures the distinct velocity correlations. The above contributions to $\langle \mathbf{J_I}(0)\mathbf{J_I}(t)\rangle$ are independent of the considered reference frame, as Raineri and Friedman[28,29] and Trullas and Padro[30,31] pointed out.

$\Lambda^d_{\mathrm{ZnBr}}(t)$ could be further subdivided into distinct velocity correlation functions according to

$$\Lambda^d_{\mathrm{ZnBr}}(t) = \frac{q_{\mathrm{Zn}}}{q_{\mathrm{Br}}}N_{\mathrm{Zn}}\left\langle \mathbf{v}_{\mathbf{i}_{\mathrm{Zn}}}(0)\sum_{j(\mathrm{Zn})\neq i}\mathbf{v}_{\mathbf{j}}(t)\right\rangle + \frac{q_{\mathrm{Br}}}{q_{\mathrm{Zn}}}N_{\mathrm{Br}}\left\langle \mathbf{v}_{\mathbf{i}_{\mathrm{Br}}}(0)\sum_{j(\mathrm{Br})\neq i}\mathbf{v}_{\mathbf{j}}(t)\right\rangle + 2\left\langle \sum_{i(\mathrm{Zn})}\mathbf{v}_{\mathbf{i}}(0)\sum_{j(\mathrm{Br})}\mathrm{v}_{\mathrm{j}}(t)\right\rangle. \tag{38}$$

However, the simulations by Trullas and Padro[31] show that the shapes of all the distinct velocity correlation functions on the right-hand side of this equation are mainly determined by the choice of the reference frame and hardly by the dynamic cross correlations between different particles. Consequently, there is no point in presenting the subdivision of $\Lambda^d_{\mathrm{ZnBr}}(t)$ into these correlation functions since $\Lambda^d_{\mathrm{ZnBr}}(t)$ itself captures the effects of distinct velocity correlations in a reference frame independent way.

Figure 3 presents the dissection of $\langle \mathbf{J_I}(0)\mathbf{J_I}(t)\rangle$ according to Eq. (37). Since the Br^- ions are the heaviest particles in the system, their velocity autocorrelation function has the longest correlation time and shows only a negligible amount of backscattering (as indicated by negative values of the correlation function). On the other hand, the Zn^{2+} ions—being lighter than the Br^- ions—give rise to a velocity autocorrelation function that decays rather rapidly and shows a complicated peak pattern and the oscillatory behavior that is characteristic for ions that are trapped inside a rigid coordination cage.[9,13]

Most noteworthy, however, is the role of the distinct velocity correlation function $\Lambda^d_{\mathrm{ZnBr}}(t)$. First, its static value vanishes, as required by theoretical predictions.[30] Second, it has a considerable influence on the current autocorrelation function, which proves that dynamic cross correlations are very pronounced in $ZnBr_2\cdot 3H_2O$ and that this system is far from being ideal in the thermodynamic sense (cf. also Sec. III D). This supports results by Chandra *et al.*,[9] who noticed

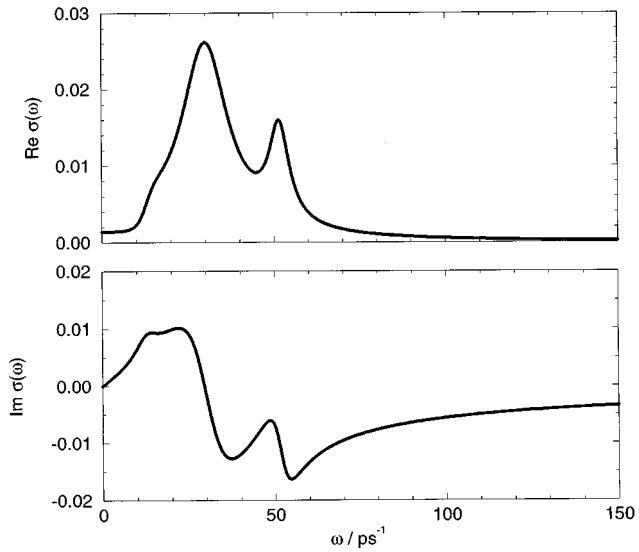

FIG. 4. Real (top graph) and imaginary (bottom graph) part of the frequency-dependent conductivity of $ZnBr_2 \cdot 3H_2O$.

in their simulations that for dense and/or highly charged ionic solutions, the peak pattern of the current autocorrelation function is different from that of the velocity autocorrelation functions—as opposed to dilute solutions, where current and velocity autocorrelation functions show an identical peak pattern.

C. The frequency-dependent conductivity $\sigma(\omega)$

According to Eqs. (33) and (12), the cross-correlation function $\langle \mathbf{M_W}(0)\mathbf{J_I}(t)\rangle$ (shown in Fig. 1) and the autocorrelation function $\langle \mathbf{J_I}(0)\mathbf{J_I}(t)\rangle$ (shown in Fig. 3) determine the frequency-dependent conductivity $\sigma(\omega)$.

Since the terms involving the cross-correlation function do not contribute to the conductivity, the formula for its calculation is simplified to

$$\sigma(\omega)=\frac{1}{3VkT}\int_0^\infty \langle \mathbf{J_I}(0)\mathbf{J_I}(t)\rangle e^{-i\omega t}dt. \tag{39}$$

The result for $ZnBr_2 \cdot 3H_2O$ is shown in Fig. 4. These results were obtained by representing the current autocorrelation function $\langle \mathbf{J_I}(0)\mathbf{J_I}(t)\rangle$ as the (perfect) fit

$$\begin{aligned}\langle \mathbf{J_I}(0)\mathbf{J_I}(t)\rangle \approx{}& 27.152\ \cos(51.568t)e^{-3.5545t}\\ &-8.7920\ \sin(12.742t)e^{-3.9755t}\\ &+126.88\ \sin(-29.974t\\ &+1.5579)e^{-8.1977t},\end{aligned} \tag{40}$$

and working with this analytical expression.

The *static conductivity*—$\sigma(\omega=0)$—is very small, which deserves a closer examination. When applying a static ($\omega=0$) electric field to a highly diluted ionic solution, we expect a quasi-independent movement of the oppositely charged ions into opposite directions, leading to a high static conductivity. In contrast to that, $ZnBr_2 \cdot 3H_2O$ is characterized by an extremely strong coupling of the collective and individual movement of the ionic species as can be judged by the importance of the distinct velocity correlation function $\Lambda^d_{\mathrm{ZnBr}}(t)$ in Fig. 3. In other words, independent motion of the ionic species in $ZnBr_2 \cdot 3H_2O$ does not exist. We have shown elsewhere[14] that the dominant coordination of Zn^{2+} ions in $ZnBr_2 \cdot 3H_2O$ consists of a central Zn^{2+} ion that is (octahedrally, in the ideal case) surrounded by four O atoms of water molecules and two Br^- ions. The fact that this coordination type is electrically neutral lends itself to a very natural explanation of the low static conductivity of $ZnBr_2 \cdot 3H_2O$: In the presence of (a moderately strong) static electric field, these neutral associations of Zn^{2+} and Br^- ions remain stable and hence do not contribute to the static conductivity. The static conductivity that is observed can be attributed either to free Zn^{2+} and Br^- ions or to charged ionic associations. But even free ions are restrained by the very strong coupling to each other and are not allowed to move independently.

As the frequency of the electric field is increased, the distinguishing properties (mass, charge, and size) of Zn^{2+} and Br^- ions lead to a disruption of ionic associations and hence the conductivity increases. Thus it seems only logical that we observe more than one dispersion peak in $\sigma(\omega)$, since there exists a plethora of different possibilities for associations in $ZnBr_2 \cdot 3H_2O$, that all show different mobilities as a complete entity and different tendencies for disruption under an electric field that varies with time.

The overall characteristics—the general tendency of the curves without the fine structure—of the frequency-dependent conductivity we observed for $ZnBr_2 \cdot 3H_2O$ are supported by a calculation of Chandra, Wei, and Patey on a model system of highly charged ions in a nonpolarizable solvent.[9]

D. Nernst–Einstein behavior and degree of ion association

The *Nernst–Einstein relation* for the calculation of the static conductivity σ ($\omega=0$) from the self-diffusion coefficients D_{Zn} and D_{Br} of the ions can be supplemented with a parameter Δ, that describes the degree of ion association in the system:

$$\sigma(0)=\frac{1}{kT}\,(q^2_{\mathrm{Zn}}\rho_{\mathrm{Zn}}D_{\mathrm{Zn}}+q^2_{\mathrm{Br}}\rho_{\mathrm{Br}}D_{\mathrm{Br}})(1-\Delta). \tag{41}$$

(ρ_{Zn} and ρ_{Br} are the number densities of the Zn^{2+} and Br^- ions, respectively.) Δ may vary between zero (pure Nernst–Einstein behavior, where ions are totally dissociated and consequently the static conductivity is completely determined by the diffusion of these ions) and one (complete ion association which results in a static conductivity of zero). The fact that the static conductivity of $ZnBr_2 \cdot 3H_2O$ is very low hints at a value of Δ which is close to one. The self-diffusion coefficients can be calculated from the velocity autocorrelation function of each ion species according to

$$D_{\mathrm{Ion}}=\tfrac{1}{3}\int_0^\infty \langle \mathbf{v}_{\mathbf{i}_{\mathrm{Ion}}}(0)\mathbf{v}_{\mathbf{i}_{\mathrm{Ion}}}(t)\rangle dt. \tag{42}$$

TABLE II. Self-diffusion coefficients, static conductivity, and resulting association parameter.

$D_{Zn}/10^{-4}\,nm^2\,ps^{-1}$	$D_{Br}/10^{-4}\,nm^2\,ps^{-1}$	$\sigma(0)/10^{-4}$	Δ
3.32	3.24	13.97	0.7

Table II collects the self-diffusion coefficients as calculated according to Eq. (42) using the velocity autocorrelation functions shown in Fig. 3, the static conductivity as accessible from Fig. 4, and the resulting parameter Δ calculated from Eq. (41). The value $\Delta=0.7$ suggests—in accordance to the observations described above—that the remnant charge transport in the case of a static external field is partly due to a small fraction of free charges.

The parameter Δ is of course closely linked to the distinct velocity correlation function $\Lambda^d_{ZnBr}(t)$ (shown in Fig. 3), as can be seen by inserting $\omega=0$ into Eq. (39) and subdividing the current autocorrelation function $\langle \mathbf{J_I}(0)\mathbf{J_I}(t)\rangle$ according to Eq. (37):

$$\sigma(0)=\frac{1}{3VkT}\left(q_{Zn}^2 N_{Zn}\int_0^\infty \langle \mathbf{v}_{Zn}(0)\mathbf{v}_{Zn}(t)\rangle dt + q_{Br}^2 N_{Br}\int_0^\infty \langle \mathbf{v}_{Br}(0)\mathbf{v}_{Br}(t)\rangle dt + q_{Zn}q_{Br}\int_0^\infty \Lambda^d_{ZnBr}(t)dt\right). \quad (43)$$

Comparing this equation to Eqs. (41) and (42) gives the following expression for Δ:

$$\Delta=-\frac{(1/V)q_{Zn}q_{Br}D^d_{ZnBr}}{q_{Zn}^2\rho_{Zn}D_{Zn}+q_{Br}^2\,\rho_{Br}D_{Br}}, \quad (44)$$

where D^d_{ZnBr} designates the distinct diffusion coefficient that is defined in analogy to Eq. (42) via

$$D^d_{ZnBr}=\tfrac{1}{3}\int_0^\infty \Lambda^d_{ZnBr}(t)dt. \quad (45)$$

Relation (44) exposes yet another facet of the distinct velocity correlation function $\Lambda^d_{ZnBr}(t)$, which is so prominent in this system: The integral $\frac{1}{3}\int_0^\infty \Lambda^d_{ZnBr}(t)dt$ is, according to Eq. (44), highly negative. Equation (43) shows that only this negative integral is responsible for the low static conductivity of $ZnBr_2\cdot 3H_2O$ because the integrals over the velocity antocorrelation functions are strictly positive.

IV. SUMMARY

We reviewed the theory of Caillol *et al.*[1,4] for the calculation of the frequency-dependent dielectric constant and the frequency-dependent conductivity of ionic solutions from MD simulations. Herein we characterized the exact treatment of the electrostatic interactions in the simulation with just one scalar parameter ϵ_{RF}.

We applied this theory to the calculation of the frequency-dependent conductivity of a saturated solution of $ZnBr_2$ in water from a 2.2-ns MD simulation employing the SPC water model. In accordance with other simulations,[8] we found the cross-correlation function $\langle \mathbf{M_W}(0)\mathbf{J_I}(t)\rangle$ to be essentially zero, and explained this by the mutual extinction of the contributions of the Zn^{2+} and Br^- ions.

We dissected the current autocorrelation function $\langle \mathbf{J_I}(0)\mathbf{J_I}(t)\rangle$ into reference frame independent correlation functions and found that not only the velocity autocorrelation functions of the two ionic species but also the distinct velocity correlations play an important role in determining the shape of $\langle \mathbf{J_I}(0)\mathbf{J_I}(t)\rangle$. We calculated the frequency-dependent conductivity of the system and found two dispersion peaks, which we attributed to the different dynamical behavior of different ion clusters in the system. We found the static conductivity to be very low and explained this with the existence of electrically neutral ion clusters consisting of one central Zn^{2+} ion surrounded by two Br^- ions and four water molecules, as these ion clusters were observed in an earlier study.[14] In accordance with the low static conductivity, we calculated a formal degree of ion association of 70% deviation from the ideal Nernst–Einstein behavior and we related this deviation parameter to the distinct velocity correlations.

ACKNOWLEDGMENT

This work was funded by the Austrian 'Fonds zur Förderung der wissenschaftlichen Forschung' under Project No. P10095-CHE.

[1] J. M. Caillol, D. Levesque, and J. J. Weis, J. Chem. Phys. **85**, 6645 (1986).
[2] J. M. Caillol, Europhys. Lett. **4**, 159 (1987).
[3] J. M. Caillol, D. Levesque, J. J. Weis, P. G. Kusalik, and G. N. Patey, Mol. Phys. **62**, 461 (1987).
[4] J. M. Caillol, D. Levesque, and J. J. Weis, J. Chem. Phys. **91**, 5544 (1989).
[5] J. M. Caillol, D. Levesque, and J. J. Weis, J. Chem. Phys. **91**, 5555 (1989).
[6] D. Levesque, J. M. Caillol, and J. J. Weis, J. Phys., Condens. Matter **2**, SA143 (1990).
[7] D. Wei and G. N. Patey, J. Chem. Phys. **94**, 6795 (1991).
[8] A. Chandra, D. Wei, and G. N. Patey, J. Chem. Phys. **98**, 4959 (1993).
[9] A. Chandra, D. Wei, and G. N. Patey, J. Chem. Phys. **99**, 2083 (1993).
[10] A. Chandra and G. N. Patey, J. Chem. Phys. **100**, 8385 (1994).
[11] J. Anderson, J. Ullo, and S. Yip, Chem. Phys. Lett. **152**, 447 (1988).
[12] H. J. C. Berendsen, J. P. M. Postma, W. F. van Gunsteren, and J. Hermans, in *Intermolecular Forces*, edited by B. Pullman (Reidel, Dordrecht, 1981), pp. 331–342.
[13] V. A. Payne, M. Forsyth, M. A. Ratner, D. F. Shriver, and S. W. de Leeuw, J. Chem. Phys. **100**, 5201 (1994).
[14] G. Löffler, T. Mager, C. Gerner, H. Schreiber, H. Bertagnolli, and O. Steinhauser, J. Chem. Phys. **104**, 7239 (1996).
[15] M. Neumann and O. Steinhauser, Chem. Phys. Lett. **95**, 417 (1983).
[16] M. Neumann and O. Steinhauser, Chem. Phys. Lett. **102**, 508 (1983).
[17] M. Neumann, O. Steinhauser, and G. S. Pawley, Mol. Phys. **52**, 97 (1984).
[18] F. Kohler, *The Liquid State* (Verlag Chemie, Weinheim, 1972), Chap. 9.2, pp. 157–167.
[19] H. J. C. Berendsen, J. P. M. Postma, A. DiNola, and J. R. Haak, J. Chem. Phys. **81**, 3684 (1984).
[20] G. Löffler, H. Schreiber, and Steinhauser (unpublished).
[21] P. P. Ewald, Ann. Phys. **64**, 253 (1921).
[22] D. J. Adams and G. S. Dubey, J. Comput. Phys. **72**, 156 (1987).
[23] S. W. de Leeuw, J. W. Perram, and E. R. Smith, Proc. R. Soc. London, Ser. A **373**, 27 (1980).
[24] W. F. van Gunsteren and H. J. C. Berendsen, *GROningen MOlecular Simulation (GROMOS) Library Manual* (Groningen, The Netherlands, 1987).

[25] J. D. Bernal and S. V. King, *Physics of Simple Liquids* (North Holland, Amsterdam, 1968).
[26] M. Neumann, F. J. Vesely, O. Steinhauser, and P. Schuster, Mol. Phys. **37**, 1725 (1979).
[27] G. F. Voronoi, J. Reine Angew. Math. **134**, 198 (1908).
[28] F. O. Raineri and H. L. Friedman, J. Chem. Phys. **91**, 5633 (1989).
[29] F. O. Raineri and H. L. Friedman, J. Chem. Phys. **91**, 5642 (1989).
[30] J. Trullas and J. A. Padro, J. Chem. Phys. **99**, 3983 (1993).
[31] J. Trullas and J. A. Padro, Phys. Rev. E **50**, 1162 (1994).